

# Electrostatic Screening and Energy Barriers of Ions in Low-dielectric Membranes

A. G. Cherstvy\*

Max-Planck-Institut für Physik komplexer Systeme, Nöthnitzerstrasse 38, D-01187 Dresden, Germany

Received: March 21, 2006; In Final Form: May 22, 2006

We present exact solutions of the linear Poisson–Boltzmann equation for several problems relevant for ion translocation across low-dielectric membranes. Our results are obtained for a finite Debye screening length, and they generalize the classical results for pure Coulombic electrostatics (Parsegian, A. *Nature (London)* **1969**, 221, 844). We calculate the electrostatic self-energy of an ion in the middle of a low-dielectric slab, its energy inside a cylindrical high-dielectric pore, and its energy inside a high-dielectric spherical jacket. We consider also the influence of negative charges distributed on the walls of the cylindrical pore. We show that ion self-energy barriers are considerably reduced due to screening of electrolyte. We compare our results with some numerical results for screened electrostatics of ion channels and wide pores.

## I. Introduction

Ion translocation across cellular membranes is known to control a number of biological processes. In a low-dielectric, hardly polarizable environment of lipid membranes ( $\epsilon_c \sim 2$ –5), the ion electrostatic self-energy (polarization or charging energy)<sup>1</sup>

$$E_c = e_0^2/(2\epsilon_c a) \quad (1)$$

can increase up to several dozens of  $k_B T$  (here  $a$  is the ion radius and  $e_0$  is the elementary charge). These unrealistically high barriers would almost block ionic current across the *bare* membranes. However, ion-transport proteins with a proper structure, which are incorporated into cell membranes, promote ion transport and allow an efficient ion permeation. Nature uses several mechanisms to decrease the electrostatic energy barriers for ion translocation and to facilitate ionic transport. In potassium channels, for instance,  $K^+$  ions in the middle of the membrane are surrounded by  $\sim 10$  Å diameter water-filled cavity.<sup>2</sup> This cavity is connected to the cytoplasm via a cylindrical water-filled pore. Second, oriented pore  $\alpha$ -helices point their partial negative charges toward this water cavity and further stabilize  $K^+$  inside the cavity. Third, in the selectivity filter of K-channels, the carbonyl oxygens of the side chains represent closely spaced 4–5 sites for  $K^+$  binding. In these sites, eight partially negatively charged oxygens surround each  $K^+$  in a 3.5 Å diameter and 12 Å long selectivity region, mimicking water's oxygens of the  $K^+$  hydration shell in aqueous solutions.<sup>3</sup> That diminishes the cost of K-dehydration necessary to enter the channel interior.<sup>4</sup> These negative charges on the pore walls provide an attractive potential for  $K^+$  entering the pore. The balance of  $K^+$  attraction to the pore walls and the repulsion of  $K^+$  ions localized in the pore was suggested to be the reason for the astonishingly high traffic rates of  $K^+$  through K-channels.<sup>4</sup>

These mechanisms of ion stabilization inside low-dielectric membranes find their physical explanation in electrostatic interactions of ions with the membrane interior and exterior.<sup>5–14</sup> Some properties of these interactions in *narrow* cylindrical pores have been recently studied in refs 15–17, based on the quasi one-dimensional nature of the electrostatic potential inside the

channel. The effects of ion-pair formation, charges on the pore walls, and ion concentration inside the pore have been considered in these papers. As the ions of the electrolyte cannot enter narrow channels, the effect of electrostatic screening on the ion self-energy and ion conductance may not be so dramatic for such channels. However, electrolyte ions can enter *wide* biopores such as gap junctions or porins<sup>18–21</sup> and synthetic nanopores<sup>22–24</sup>—the effect of electrolyte screening is thus expected to be stronger in this case. So, in contrast to refs 15–17 where the channels have to be narrower than the Debye screening length, we concentrate here mainly on wide channels/pores. The ion self-energy should decrease due to the screening inside the pores/cavities and outside in the solution. The ion conductance across the pore is thus expected to increase faster-than-linearly with the ion concentration in solution as is typical for the bulk ionic conductance. The effect of electrolyte on the ion self-energy both for narrow (gramicidin A) and for wide (gap junction and porin) pores has been investigated numerically in ref 14 on the basis of solutions of the nonlinear Poisson–Boltzmann equation. We compare some of our analytical results with the results of that paper.

Here, we present the analytical solutions of some electrostatic problems relevant for ion translocation across membranes and wide pores in the presence of electrolyte. Our solutions generalize those of Parsegian<sup>5</sup> obtained for nonscreened Coulombic interactions. We calculate the decrease of the ion self-energy due to the Debye–Hückel screening for the following geometries: ion in the center of a low-dielectric planar slab (section II), ion in a high-dielectric cylindrical pore inside a low-dielectric medium (section III), and ion covered by a high-dielectric spherical jacket (section IV). We also study the effect of distributed charges on the walls of cylindrical pores. The graphs in each section represent the energies calculated in the same section.

## II. Slab

Let us shortly discuss some approximations used in the text. We solve the linear Poisson–Boltzmann equation assuming that the electrostatic potential is small everywhere; it is known to break down near highly charged surfaces. Water is modeled as a structureless dielectric continuum with a uniform dielectric constant; in narrow pores and close to charged surfaces, the

\* E-mail: cherstvy@pks.mpg.de.

dielectric response can however be modified due to dielectric saturation and nonlocality.<sup>25</sup> The dielectric boundary of membrane and water is considered to be sharp. In reality, however, channel-forming proteins can have a different dielectric constant than that of the membrane; see refs 8 and 12. For such a complicated dielectric boundary, the electrostatic calculations for the chosen geometries can in principle be performed analogously as is done below.

In this section, we calculate the electrostatic potential  $\varphi$  of a single pointlike ion with the charge  $e_0$  in the center of a planar slab of thickness  $L$  and with a small dielectric constant  $\epsilon_c$  surrounded by electrolyte solution with the dielectric constant of water  $\epsilon_0 \approx 80$  and reciprocal Debye screening length  $\kappa = (8\pi l_B n_0)^{1/2}$ . Here,  $l_B = e_0^2/(\epsilon_0 k_B T)$  is the Bjerrum length ( $\approx 7.1$  Å in water at room temperature), and  $n_0$  is the concentration of 1:1 salt in solution. The slab is a model for a membrane lipid bilayer, and upon translocation across such a membrane, the ion self-energy becomes maximal in its middle. Here, we calculate only this maximal energy value, not the whole shape of the self-energy profile across the membrane (see refs 14 and 15) and consider only a single ion. The membrane is considered to be neutral.<sup>26</sup> The coordinates  $x$  and  $y$  are in the slab plane;  $z$  is perpendicular to it.

The Laplace equations for distribution of the dimensionless electrostatic potential  $\psi = e_0\varphi/(k_B T)$  inside ( $\psi_c$ ) and outside ( $\psi_0$ ) the slab can be written in terms of the Fourier components  $\tilde{\psi}(k, z) = \int_{-\infty}^{\infty} \int_{-\infty}^{\infty} dk_x dk_y e^{ik_x x} e^{ik_y y} \psi(x, y, z)$  as  $d^2\tilde{\psi}_0(k, z)/dz^2 - \kappa^2\tilde{\psi}_0(k, z) = 0$  and  $d^2\tilde{\psi}_c(k, z)/dz^2 - k^2\tilde{\psi}_c(k, z) = 0$ , where  $\kappa_k = (k^2 + \kappa^2)^{1/2}$  and  $k^2 = k_x^2 + k_y^2$ . We supply these equations with the matching conditions for potential and its derivative on the dielectric boundary and with the condition  $\partial\tilde{\psi}_0(k, z)/\partial z|_{z=0} = -e_0^2/(\pi\epsilon_c k_B T)$  at the point where the charge is located. Then one can obtain

$$\tilde{\psi}_c(k, z) = \frac{l_B \epsilon_0 f(k) e^{-kz} - e^{-kL} e^{kz}}{\pi k \epsilon_c [f(k) + e^{-kL}]}$$

where

$$f(k) = \frac{\epsilon_0 \kappa_k + \epsilon_c k}{\epsilon_0 \kappa_k - \epsilon_c k} \quad (2)$$

At  $L \rightarrow \infty$  from this expression, we get the unscreened Coulombic potential  $\varphi_c(r) = e_0/(\epsilon_c |\vec{r}|)$ , where  $|\vec{r}| = (x^2 + y^2 + z^2)^{1/2}$ . The correction to the self-energy of a pointlike ion inside an infinite low-dielectric medium  $E_c$  then is

$$\Delta E(\kappa) = \frac{e_0^2}{2\epsilon_c} \int_0^\infty dk \left[ \frac{f(k) - e^{-kL}}{f(k) + e^{-kL}} - 1 \right] \quad (3)$$

The unity corresponding to  $E_c$  has been subtracted from the integrand above. At  $\kappa = 0$ , this integral gives the results of ref 5

$$\Delta E(0) = -\frac{e_0^2}{\epsilon_c L} \ln \frac{2\epsilon_0}{\epsilon_0 + \epsilon_c} \quad (4)$$

In Figure 1, we plot the ratio  $\Delta E(\kappa)/\Delta E(0)$  as a function of slab thickness  $L$ . For  $\epsilon_c/\epsilon_0 \ll 1$ , the screening of outer electrolyte solution results in a small correction to the classical result in the absence of salt. In this figure, we show for comparison by dots the results of the numerical solution of the nonlinear Poisson–Boltzmann equation obtained in ref 14 for the self-energy of 1 Å radius ion in the middle of a gramicidin-like

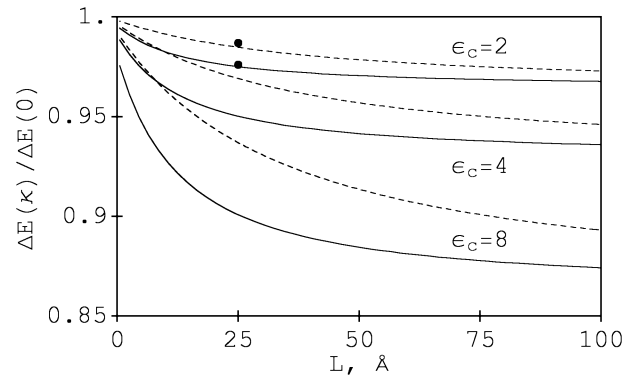


**Figure 1.** Ion self-energy in the middle of a dielectric slab surrounded by electrolyte with  $1/\kappa = 7$  Å (solid) and  $1/\kappa = 20$  Å (dashed curves). The two dots are the results of ref 14 for a gramicidin-like cylindrical channel, at the same ionic strengths and at  $\epsilon_c = 2$ .

cylindrical pore ( $L = 25$  Å and  $a = 2.5$  Å inside a planar slab with  $\epsilon_c = 2$ ). In the numerical scheme, this narrow pore contained *no* electrolyte and the screening was only due to electrolyte solution *outside* the slab. Note that, although at low salt concentrations the agreement is good, at  $n_0 \sim 1$  M, the numerical solution of ref 14 results in a slightly lower ion self-energy.

### III. Cylindrical Pore

The electrostatic potential of a positive charge  $e_0$  on the axis of an infinite high-dielectric cylindrical pore of radius  $b$  inside a low-dielectric medium is obtained below via solving the linear Poisson–Boltzmann equation inside (dielectric constant is  $\epsilon_0$  and potential is  $\varphi_0(x, r)$ ) and the Laplace equation outside the pore ( $\epsilon_c$  and  $\varphi_c(x, r)$ ). That is, we have  $\Delta\varphi_0(r, x) = \kappa^2\varphi_0(r, x) - 4\pi e_0\delta(x)\delta(r)/\epsilon_0$  and  $\Delta\varphi_c(r, x) = 0$ , where  $\delta(x)$  is the Dirac delta function. The Fourier transformation over  $x$ ,  $\psi_{0,c}(r, x) = \pi^{-1} \int_0^\infty \cos(kx) \tilde{\psi}_{0,c}(r, k) dk$ , leads to  $d^2\tilde{\varphi}_0(r, k)/dr^2 + r^{-1} d\tilde{\varphi}_0(r, k)/dr - \kappa^2\tilde{\varphi}_0(r, k) = -2e_0\delta(r)/\epsilon_0$  and  $d^2\tilde{\varphi}_c(r, k)/dr^2 + r^{-1} d\tilde{\varphi}_c(r, k)/dr - k^2\tilde{\varphi}_c(r, k) = 0$ . The general solutions of the corresponding homogeneous equations are  $\tilde{\varphi}_c(r, k) = \alpha K_0(kr) + \beta I_0(kr)$  and  $\tilde{\varphi}_0(r, k) = \gamma K_0(\kappa_k r) + \lambda I_0(\kappa_k r)$ , where  $K_0$  and  $I_0$  are the modified Bessel functions of the first order and  $r$  is the distance from the pore axis. Using the conditions of continuity of the electrostatic potential  $\tilde{\varphi}_c(r)|_{r=b} = \tilde{\varphi}_0(r)|_{r=b}$  and of the normal electric field's component,  $\epsilon_c \partial\tilde{\varphi}_c(r)/\partial r|_{r=b} = \epsilon_0 \partial\tilde{\varphi}_0(r)/\partial r|_{r=b}$ , putting  $r \partial\tilde{\varphi}_0(r)/\partial r|_{r=0} = -2e_0/\epsilon_0$ , and using the potential decay far from the charge that leads to  $\beta = 0$ , one finds coefficients  $\alpha$ ,  $\gamma$ , and  $\lambda$  and obtains for the Fourier components

$$\tilde{\varphi}_0(r, k) = 2e_0 [K_0(\kappa_k r) + F(k, \kappa) I_0(\kappa_k r)]/\epsilon_0, \quad (5)$$

$$\tilde{\varphi}_c(r, k) = \frac{2e_0 K_0(kr)/b}{\epsilon_0 \kappa_k I_1(\kappa_k b) K_0(kb) + \epsilon_c k K_1(kb) I_0(\kappa_k b)} \quad (6)$$

where

$$F(k, \kappa) = \frac{\epsilon_0 \kappa_k K_1(\kappa_k b) K_0(kb) - \epsilon_c k K_1(kb) K_0(\kappa_k b)}{\epsilon_0 \kappa_k I_1(\kappa_k b) K_0(kb) + \epsilon_c k K_1(kb) I_0(\kappa_k b)} \quad (7)$$

The first term in the expression for  $\tilde{\varphi}_0(r, k)$  corresponds to the screened potential of an ion in electrolyte solution,  $\varphi_0 = e_0 e^{-\kappa|\vec{r}|}/\epsilon_0 |\vec{r}|$ , which at  $\kappa \rightarrow 0$  gives the classical result,  $E_0 = e_0^2/(2\epsilon_0 a)$ . The second term in  $\tilde{\varphi}_0(r, k)$  emerges due to the dielectric boundary; see also ref 17. The ion self-energy can then be written as

$$E(\kappa) = \frac{e_0^2}{\epsilon_0 \pi} \left[ \int_0^{1/a} K_0(\kappa_k r) dk + \int_0^\infty F(k, \kappa) dk \right] \quad (8)$$

The correction to  $E_0$  due to the dielectric boundary (second term in this equation) is calculated here as for a pointlike ion; see ref 28. At  $\kappa = 0$ , the ion self-energy turns into that obtained by Parsegian<sup>5</sup>

$$E(0) = E_0 + e_0^2 P(\epsilon_c/\epsilon_0)/\epsilon_c b \quad (9)$$

where  $P(\epsilon_c/\epsilon_0)$  is the tabulated function with a maximum at  $\epsilon_c/\epsilon_0 \approx 0.2$ ; see Figure 2 in ref 5 (see also a more elaborate consideration of ion charging energy in cylindrical geometry in ref 29, including the treatment of nonlocal electrostatics). At a finite  $\kappa$ , the electrolyte screening diminishes the ion self-energy dramatically; see Figure 2. We use below  $a = 1 \text{ \AA}$  as a typical ionic radius ( $a_{K^+} = 1.33 \text{ \AA}$ ,  $a_{Na^+} = 0.95 \text{ \AA}$ ).

In this figure, we show for comparison the results of Jordan et. al.<sup>14</sup> for the decrease of ion self-energy with salt concentration in an *E.coli* porin-like cylindrical pore ( $L = 55 \text{ \AA}$ ,  $b = 6 \text{ \AA}$ ,  $\epsilon_c = 2$ ). Similarly to our model, the electrolyte was assumed to fill this relatively wide pore and to shield the influence of the low-dielectric membrane core. In simulations, the outer electrolyte contributes to the screening as well and this can be one of the reasons why the ion self-energy decreases considerably faster with the increase of  $\kappa$  in simulations than in our model, where the pore is infinite and the screening is solely due to the electrolyte inside the pore. Note here that the problem of ion self-energy in a pore with a *finite* length in a low-dielectric membrane has no simple answer; see refs 7, 9, and 17. The “sum” of the corrections (4) and (9) for the dielectric slab without a pore and for an infinite cylindrical pore was shown to overestimate the real value of the Born charging energy.<sup>7</sup>

Let us consider now an equidistant array of positive charges inside a cylindrical high- $\epsilon$  pore; the pore walls are charged with the uniform charge density  $\sigma < 0$ . The positive charges are assumed to be positioned on the pore axis minimizing the influence of low- $\epsilon$  walls on the ion self-energy (although such a positioning might not be optimal from the point of view of interaction of charges with the pore walls, see ref 30). The Fourier transformation that accounts for the charge periodicity is  $\tilde{\varphi}_{c,0}(r, n) = h^{-1} \int_{-h/2}^{h/2} e^{ingx} \varphi_{c,0}(r, x) dx$ , where  $g = 2\pi/h$  and  $h$  is the charge–charge separation in the array. Similar to the previous section, applying  $\tilde{\varphi}_c(r)|_{r=b} = \tilde{\varphi}_0(r)|_{r=b}$ ,  $\epsilon_c \partial \tilde{\varphi}_c(r)/\partial r|_{r=b} - \epsilon_0 \partial \tilde{\varphi}_0(r)/\partial r|_{r=b} = -4\pi\sigma\delta_{n,0}$  and  $r \partial \tilde{\varphi}_0(r)/\partial r|_{r=0} = -2e_0/(\epsilon_0 h)$ , we can obtain

$$\tilde{\varphi}_0(r, n) = 2e_0 K_0(\kappa_n r)/(\epsilon_0 h) + 2J_n I_0(\kappa_n r) \quad (10)$$

where

$$J_n = \{2\pi\sigma\delta_{n,0}K_0(ngb) + e_0[\epsilon_0\kappa_n K_1(\kappa_n b)K_0(ngb) - \epsilon_c ng K_1(ngb)K_0(\kappa_n b)]/(\epsilon_0 h)\}/[\epsilon_0\kappa_n I_1(\kappa_n b)K_0(ngb) + \epsilon_c ng K_1(ngb)I_0(\kappa_n b)] \quad (11)$$

Here,  $\kappa_n = (\kappa^2 + n^2 g^2)^{1/2}$  and  $\delta_{n,0}$  is the Kronecker delta. We see that only the uniform component of the electrostatic potential depends on the wall charge density  $\sigma$ . Note that from this expression one can obtain the potential of this periodic charge

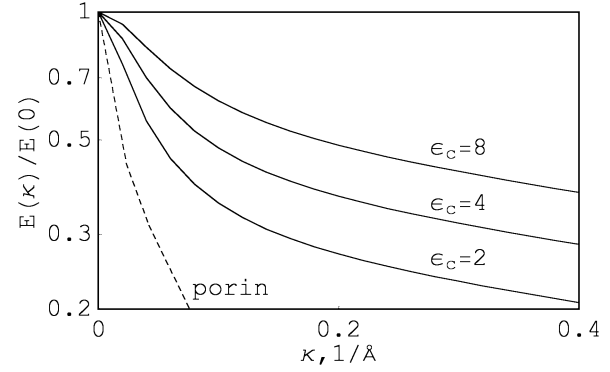


**Figure 2.** Ion self-energy inside an infinite cylindrical pore at  $a = 1$  and  $b = 6 \text{ \AA}$ . At larger  $\kappa a$ , the theoretical curves  $\propto e^{-\kappa a}$ . The results of ref 14 for a porin-like channel are plotted as the dotted curve.

array in electrolyte without dielectric boundaries

$$\psi_0(r, x) = e_0 \sum_{n=-\infty}^{\infty} e^{-ingx} \tilde{\varphi}_0(r, n)/(k_B T) = 2\xi K_0(\kappa r) + 4\xi \sum_{n=1}^{\infty} \cos(ngx) K_0(\kappa_n r) \quad (12)$$

where  $\xi = l_B/h$  is Manning's charge parameter.<sup>31</sup>

For the values of parameters relevant to some ion channels ( $b \sim 5 \text{ \AA}$ ,  $\epsilon_c \sim 2$ ,  $\kappa \sim 1/10 \text{ \AA}^{-1}$ ), the values of  $J_n$  decay fast with  $n$ . The  $J_0$  vanishes when the magnitude of the wall charge density is  $\sigma^* = -e_0\kappa K_1(\kappa b)/(2\pi h)$ . That means that in the limit of small  $\kappa$  the ions in the pore are totally neutralized by the negative wall charges, whereas the  $\sigma^*$  required decreases with  $\kappa$ . A similar conclusion about the *pore neutrality* has been suggested recently by Shklovskii et. al.<sup>15</sup> as a reason for the decrease in the ion self-energy in the pore. The correction to the self-energy of one charge of the array in the pore (as compared with its energy in the periodic charge array in a high- $\epsilon$  electrolyte) is dominated by the  $n = 0$  term of the sum,  $\Delta E = \sum_{n=-\infty}^{\infty} e_0 J_n$ . In the limit of infinitely separated charges in the noncharged pore without screening ( $\sigma = 0$ ,  $\kappa = 0$ ,  $h \rightarrow \infty$ ;  $J_n$  values decay slowly with  $n$ ), the correction  $\Delta E$  turns into that obtained by Parsegian,  $\Delta E = e_0^2 \epsilon_0^{-1} \pi^{-1} \int_0^\infty F(k, 0) dk$ ; see Figure 2 in ref 5.

#### IV. Spherical Jacket

Consider a spherical jacket of radius  $b$  with the dielectric constant  $\epsilon_0$  around an ion of radius  $a$ ; outside the jacket the dielectric constant is  $\epsilon_c$ . Inside the jacket we solve  $\Delta\psi_0(r) = \kappa^2\psi_0(r)$  with the general solutions in the form  $e^{\pm\kappa r}/r$ . Outside the jacket the  $1/r$  Coulombic potential solves the Laplace equation. Matching potentials and their derivatives at  $r = b$ , one can obtain

$$\varphi_0(r) = \frac{e_0 e^{-\kappa a} (\kappa b + 1 - \epsilon_c/\epsilon_0) e^{-2\kappa b} e^{\kappa r} + (\kappa b - 1 + \epsilon_c/\epsilon_0) e^{-\kappa r}}{\epsilon_0 r m(\kappa)}$$

$$\varphi_c(r) = \frac{e_0 e^{-\kappa a} 2\kappa b e^{-\kappa b}}{\epsilon_0 r m(\kappa)} \quad (13)$$

where  $m(\kappa) = (\kappa a + 1)(\kappa b - 1 + \epsilon_c/\epsilon_0) e^{-2\kappa a} - (\kappa a - 1)(\kappa b + 1 - \epsilon_c/\epsilon_0) e^{-2\kappa b}$ . The ion self-energy is obtained as  $E(\kappa) =$

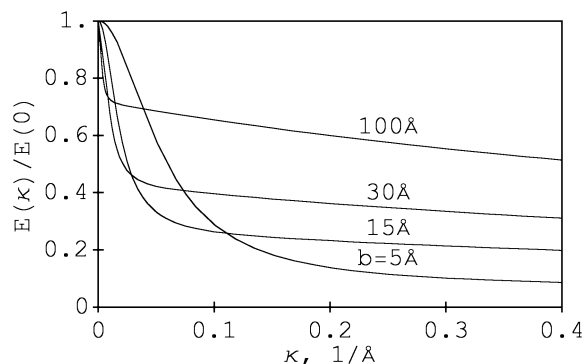


**Figure 3.** Ion self-energy inside a spherical electrolyte-filled jacket at  $a = 1 \text{ \AA}$  and  $\epsilon_s = 2$ .

$e_0\phi_0(a)/2$ . For  $\kappa = 0$ , we obtain the result of Parsegian<sup>5</sup>

$$E(0) = E_0 + e_0^2(1/\epsilon_c - 1/\epsilon_0)/2b \quad (14)$$

whereas the ion self-energy considerably decreases with  $\kappa$ ; see Figure 3. For large jackets, as one could expect, the ion self-energy approaches its value in the bulk electrolyte,  $E(\kappa) = E_0/(1 + \kappa a)$ .

## V. Discussion

We have considered the effect of electrolyte effect on the electrostatic energy barriers for ion allocation in low-dielectric membranes, cylindrical pores, and spherical jackets. In the two latter cases, we found a considerable decrease of ion self-energy as compared with the pure Coulombic result. This decrease in ion self-energy can result in an increase in ion conductance of cylindrical channels at higher ion concentrations in solution. Although our mean-field results cannot be directly applied to narrow cylindrical single-file channels/pores (such as gramicidin A, potassium, or sodium channels which are smaller than  $1/\kappa$  or  $\sim 10 \text{ \AA}$ ), they can be relevant for wide biological pores (such as porin or gap junctions) which *can* be filled with electrolyte, particularly at high salt concentrations. Indeed, the ionic conductance of porin increases dramatically with the salt concentration<sup>20</sup> (almost linearly in log–log plot, see Figure 6 in ref 32). Also, the ion selectivity of the OmpF porin was shown to decrease considerably at nearly molar salt that has been attributed to screening of the electrostatic field of pore protein charged residues.<sup>21</sup> The conductance of some synthetic nanopores of 2–10 nm in diameter also increases with the ionic strength in solution; see, for example, Figure 5 in ref 23 and Figure 2b in ref 24.

Our simple continuum mean-field model however neglects many important properties of realistic ion channels. More advanced models for studying static and dynamic properties of model ion channels have to be developed to treat such important effects as (a) ion size and channel selectivity, (b) the distribution of the pore charges, the effects of their discreteness, and the dependence of their magnitude on salt concentration,<sup>33</sup> (c) ion–channel interactions upon ion translocation and thermodynamic

equilibrium of ions in the pore with solution (the Donnan equilibrium, see, e.g., ref 21), (d) ion–ion interactions when several ions are bound in the pore,<sup>10,11,13</sup> (e) the shape of the channel and the profile of the dielectric constant, (f) water structuring in pores and ion hydration, and (g) pore and membrane deformability/adjustability. This can be the subject of further investigations of electrostatic interactions on nanoscale.

## References and Notes

- (1) Born, M. *Z. Phys.* **1920**, *1*, 45.
- (2) Doyle, D. A.; et al. *Science* **1998**, *280*, 69.
- (3) Zhou, Y.; et al. *Nature (London)* **2001**, *414*, 43.
- (4) Morais-Cabral, J. H.; Zhou, Y.; MacKinnon, R. *Nature (London)* **2001**, *414*, 37.
- (5) Parsegian, A. *Nature (London)* **1969**, *221*, 844.
- (6) Parsegian, A. *Ann. N. Y. Acad. Sci.* **1975**, *264*, 161.
- (7) Levitt, D. G. *Biophys. J.* **1978**, *22*, 209.
- (8) Jordan, P. C. *Biophys. Chem.* **1981**, *13*, 203.
- (9) Jordan, P. C. *Biophys. J.* **1982**, *39*, 157.
- (10) Levitt, D. G. *Biophys. J.* **1985**, *48*, 19.
- (11) Chizmadjev, Yu. A.; Aityan, S. Kh. *J. Theor. Biol.* **1977**, *64*, 429.
- (12) Koumanov, A.; et al. *Eur. Biophys. J.* **2003**, *32*, 689.
- (13) Cheng, M. H.; Coalson, R. D. *J. Phys. Chem. B* **2005**, *10*, 488.
- (14) Jordan, P. C.; et al. *Biophys. J.* **1989**, *55*, 1041.
- (15) Zhang, J.; Kamenev, A.; Shklovskii, B. *Phys. Rev. Lett.* **2005**, *95*, 148101.
- (16) Kamenev, A.; et al. *Physica A* **2006**, *359*, 129 and references therein.
- (17) Teber, S. *J. Stat. Mech.* **2005**, *7*, P07001.
- (18) Finkelstein, A. *Ann. N. Y. Acad. Sci.* **1985**, *456*, 26 and references therein.
- (19) Karshikoff, A.; et al. *J. Mol. Biol.* **1994**, *240*, 372.
- (20) Nestorovich, E. M.; et al. *Biophys. J.* **2003**, *85*, 3718.
- (21) Alcaraz, A.; et al. *Biophys. J.* **2004**, *87*, 943.
- (22) Siwy, Z.; et al. *Phys. Rev. Lett.* **2005**, *94*, 048102.
- (23) Ho, C.; et al. *Proc. Natl. Acad. Sci. U.S.A.* **2005**, *102*, 10445.
- (24) Smeets, R. M. M.; et al. *Nano Lett.* **2006**, *6*, 89.
- (25) Bopp, Ph. A.; Kornyshev, A. A.; Sutmman, G. *Phys. Rev. Lett.* **1996**, *76*, 1280.
- (26) Kornyshev, A. A. *Electrochim. Acta* **1981**, *26*, 1.
- (27) When the density of negatively charged membrane lipids increases, the ion conductance of some bilayer-incorporated ion channels including gramicidin A and porin increases as well due to a higher concentration of positive ions near the channel mouth and thus a higher probability for an ion to enter the channel; see discussion in refs 21 and 27.
- (28) Rostovtseva, T. K.; et al. *Biophys. J.* **1998**, *75*, 1783.
- (29) The analysis of the electrostatic problem of a *finite-size* polarizable ion sphere inside a water-filled cylindrical pore in a low-dielectric membrane has been performed in ref 8. It was shown that for realistic ratios of ion radii to pore radii the correction to the self-energy due to the ion size is negligible, as compared with the results of Parsegian for a pointlike ion.<sup>5</sup>
- (30) Kornyshev, A. A.; Vorotyntsev, M. A. *J. Phys. C: Solid State Phys.* **1979**, *12*, 4939.
- (31) Warshel, A.; Russel, S. T.; Churg, A. K. *Proc. Natl. Acad. Sci. U.S.A.* **1984**, *81*, 4785.
- (32) Manning, G. S. *Q. Rev. Biophys.* **1979**, *11*, 179. See also Cherstvy, A. G.; Leikin, S.; Kornyshev, A. A. *J. Phys. Chem. B* **2002**, *106*, 13362. Cherstvy, A. G.; Leikin, S.; Kornyshev, A. A. *J. Phys. Chem. B* **2004**, *108*, 6508.
- (33) Mathes, A.; Engelhardt, H. *Biophys. J.* **1998**, *75*, 1255 and references therein.
- (34) For instance, for Ca-activated K-channels, the conductance was shown to *decrease* as the concentration of mono- and divalent cations in solution grows.<sup>34</sup> It was suggested that salt ions can screen the pore charges diminishing the translocation rates (although the “ion blockage” mechanism cannot be completely excluded as well) indicating a possible 2-fold role of salt in solution on the conductivity of these channels.
- (35) MacKinnon, R.; LaTorre, R.; Miller, C. *Biochemistry* **1989**, *28*, 8092.